Open Access Article
The authors, the publisher, and the right holders grant the right to use, reproduce, and disseminate the work in digital form to all users.

Technology in Cancer Research & Treatment
ISSN 1533-0346
Volume 2, Number 6, December (2003)
Adenine Press

Dynamic Infrared Imaging of Newly Diagnosed Malignant Lymphoma Compared with Gallium-67 and Fluorine-18 Fluorodeoxyglucose (FDG) Positron Emission Tomography

Milos J. Janicek, M.D., Ph.D.[1]*
George Demetri, M.D.[2]
Milos R. Janicek[3]
Kitt Shaffer, M.D., Ph.D.[1]
Mark A. Fauci, B.S.S., M.B.A.[4]

www.tcrt.org

Staging and therapy monitoring of malignant lymphomas relies heavily on imaging using arbitrary size criteria from computed tomography (CT) and sometimes non-specific radionuclide studies to assess the activity of the disease. Treatment decisions are based on early assessment of the response to therapy and the residual volume of the disease. Our initial experience is reported using a new noninvasive, inexpensive, and reproducible passive imaging modality, Dynamic Infrared Imaging (DIRI), which may add a new dimension to functional imaging. This system relies on its ability to filter the raw infrared signal using biological oscillatory behavior. It detects and analyzes minute oscillations of temperature and heat distribution in tumors.

[1]Department of Radiology
[2]Adult Oncology
Dana-Farber Cancer Institute
Brigham and Women's Hospital
Harvard Medical School
Boston, MA
[3]Williams College
Williamstown, MA
[4]OmniCorder Technologies, Inc.
12 Technology Drive
Suite 8
East Setauket, NY

Introduction

The treatment of malignant lymphomas depends heavily on imaging at the time of staging. With the progress in therapy there is an increasing demand for more frequent and accurate monitoring of the early response to treatment, as well as the detection of toxicity of chemotherapy. Early assessment of response and toxicity will allow more timely changes in the treatment of patients who are not responding, and may enhance the chances of decreasing toxic side effects and ultimately increase the prospect for a cure. Functional imaging techniques are becoming more widely accepted for this purpose, and imaging modalities using Ga-67 or FDG-PET show very promising results in this regard (1-5). Some studies suggest that very early restaging – as early as after one cycle of therapy – may be predictive of the treatment success or failure (1, 6). PET likewise, has been employed in the early monitoring of lymphoma patients on radio-immunotherapy (7). PET assessment of tumor glucose or amino acid metabolism with F-18 FDG, C-11 Thyrosin PET, C-11 cystein PET have shown very encouraging results in a variety of tumors, although larger studies are needed to confirm this concept (3, 7-9). Our report on this new imaging modality, Dynamic Infrared Imaging (DIRI) is based on our working hypothesis that tumors can be detectable as areas of long-wave (8-10μm) infrared photon flux that exhibit significantly different temporal behavior when compared to non-diseased tissue.

In this study, we compare the ability of Dynamic Infrared Imaging (DIRI) to depict tumor masses in lymphoma patients for staging and therapy monitoring against CT, Ga-67 and FDG–PET.

Staging CT, Ga-67 and FDG-PET were compared with DIRI images on ten patients (five males, five females) in age range from 25-50 years with newly

* Corresponding Author:
Milos J. Janicek, M.D., Ph.D.
Email: Milos_janicek@dfci.harvard.edu

diagnosed lymphoma. We compared the ability of DIRI to depict tumor masses in superficial locations and define characteristic patterns that could be used later for therapy monitoring. Twenty-eight tumor sites were identified using Ga-67 and/or FDG-PET and CT measurable tumor masses, amenable to a single view dynamic acquisition utilizing the BioScanIR® System (OmniCorder Technologies Inc., East Setauket, NY). Each acquisition consisted of 2048 images taken over 20 seconds. Various algorithms were used to extract and analyze the infrared data from the 28 tumor sites which were then translated to visual images and compared to 29 regions in adjacent soft tissues without tumor.

There was very close correlation in selected locations between tumor depiction by DIRI as compared to Ga-67, FDG-PET, and CT. Average temperature sampled over tumor masses within a 20 × 20 pixel region was significantly higher than those over adjacent soft tissues (31.78 ± 0.98 vs. 31.23 ± 0.71  C; P=.017, t-test), and these differences were confirmed on color-coded maps as areas of high relative temperature and high temperature modulation. Tumors showed lower raw temperature and temperature modulation with prominent high modulation rim in two patients. The semi-quantitative evaluation showed significant correlation between Ga uptake and high temperature modulation (P<.001), as well as high relative temperature (P<.001) compared to tumor sites with soft tissues outside the tumor. No consistent pattern of thermo-homogeneity was seen throughout the tumors. Raw temperature and temperature modulation measurements using DIRI are able to distinguish lymphoma from adjacent tissues.

DIRI is able to distinguish lymphoma from adjacent tissues. "Typical patterns" may be identified that may allow the incorporation of this promising functional imaging technique to monitor patients with lymphoma during therapy.

DIRI is a new infrared imaging technique that records natural infrared radiation (IR) from tissue. Living tissue continuously emits IR photons in the 8 to 10μm frequency. IR intensity is proportional to the temperature of the radiating tissue, and is indirectly proportional to the degree of tissue perfusion. DIRI has superficial similarities to a previous technique called thermography, but the means of collecting and processing the data are so different that it is described in the literature as a new and distinct modality, referred to alternatively as DIRI, HPIR or DAT (10, 11).

The first significant attempts to utilize the infrared technology in medical imaging were in the field of breast cancer diagnosis. These early attempts were hampered by inferior infrared technology, very limited data processing capability and a poor understanding of the biology of cancerous lesions. Regardless, throughout the 1960s, 70s, 80s and early 90s hundred of reports persistently indicated a correlation between the development and growth of cancerous lesions and heat emission.

Our understanding of cancer biology grew enormously in the 1980s and 90s. In1986 Ignarro reported that nitric oxide relaxes smooth muscles in the walls of blood vessels, and has a role in a range of biological processes, with possible implications in cancer research (24). In 1996 Gamagami reported infrared imaging had the ability to non-invasively monitor angiogenesis in cancerous tissue (23). In the meantime, new infrared technology became available in 1996 in the form of the first QWIP camera, developed by Gunapala at NASA's Jet Propulsion Laboratory. In 1997 Anbar reported it was possible to measure normal blood perfusion using this same QWIP camera (17). In 1999 Anbar, using a substantially more advanced QWIP camera, reported that cancerous lesions could be objectively identified (12).

MRI, CT, ultrasound and other conventional imaging modalities input and manipulate a known signal while measuring its alteration through the tissue. Conversely, DIRI detects and passively analyses infrared energy radiating from the tissue. Because DIRI is a passive imaging system, and therefore cannot control the electromagnetic signal to enhance the image analysis, the system relies on its ability to filter the raw signal using biological oscillatory behavior. Oscillation of heat emission can be analyzed for different frequencies. M. Anbar *et al*. reported on the frequency analyses predictive of breast cancer (12). Similar results were reported by T. M. Button *et al*. in his preliminary work as "vasomotor frequencies" (27). F. Meyer *et al*. reported that infrared flux rates of change – or slope analysis – are useful in monitoring brain function during surgery.

In this study three algorithms were used to extract and analyze the infrared data. All the information was then translated into a visual image with 256 colors. Spot averaging analysis (SAA) merged neighboring 2 × 2 or 4 × 4 pixel arrays and averaged the temperature for all frames in the acquisition. Spot Standard Deviation (SSD) measured the standard deviation of the change in temperature for a 2 × 2 array over the duration of image acquisition. A positive Spot Slope is translated into colors from the high end of the visible spectrum (white and red) for relative increase in temperature. Constant temperatures are in the middle range (green and blue). Negative slope (decrease in temperature) is shown with colors at the low end (black). The Fast Fourier Transformation (FFT) algorithm gates the frequency of known physiological processes, such as cardiac cycle, to the intensity of IR emission expressed as 'Modulation of temperature.'

Technology

DIRI records changes in perfusion and reperfusion of human tissues by rapid (>=100 frames per second) measurement of

minute changes (<0.006 degrees) in photon flux, both spatially and temporally. High spatial and temporal resolution is essential for identifying tumor masses (10, 11). The central component that provides this capability and therefore makes DIRI clinically viable is a sensor developed for the strategic defense initiative (SDI), or the "Star Wars" research program. This extraordinarily sensitive, high speed sensor is called the quantum well infrared photo detector (QWIP). The QWIP is a long wave (8-10μm), narrow band, focal plane array infrared detector. Long-wave detectors are superior for measuring biological behavior because tissue has its peak emissivity in the 8 to 10μm frequency range. Mid-wave IR detectors (3-5μm), on the other hand are subject to environmental artifacts. For example, up to 15% of the information detected in the mid-wave can be reflected by environmental sources versus <2% in the 8-10μm range. So the 8-10μm narrow band capability of the QWIP is ideal for medical imaging applications. A typical QWIP is a 256 × 256 array with 65,000 pixels per frame that can resolve a 0.006 degrees C difference in temperature over time. The QWIP's spatial resolution is 40μm, with more than 99.5% operating pixel yield. Next generation QWIP detectors offer 640 × 480 resolution (307,200 pixels) at 20μm, nearly five times the effective spatial resolution.

The QWIP detector is incorporated into a camera and built into a self-contained mobile unit that includes: a customized computer for data analysis, a LED display, a printer and a black body calibration unit. This integrated unit can collect up to 400 frames/second of data with a 14 bit digital output. The QWIP detector operates at cryogenic temperatures of approximately 60K, but the cooling operation is performed with an entirely sealed, long-life (4000+ hrs), sterling cooling system, so the handling of cryogenic liquids is eliminated. The camera is equipped with a 50mm f/2 germanium lens, but can be refitted with numerous lens configurations including microscopic and endoscopic lenses.

Materials and Methods

Our study was conducted on a group of 10 patients (five males, five females) ranging in age from 25-50 years, all of whom had newly diagnosed malignant lymphoma. Five patients had Hodgkin disease and five non-Hodgkin lymphomas affecting the neck, axillae and anterior mediastinum. The lesions were identified by computed tomography (CT) and corroborated by staging gallium-67 scans and/or fluorine-18 flouro-deoxyglucose positron emission tomography (PET). Gallium scans were performed 72 hours after injection of 370 MBq of gallium-67 citrate in all 10 patients, and included both planar and SPECT (single photon emission tomography) images recorded in the standard manner (1). PET scans were obtained from six subjects 48 minutes after injection of the 20 mCi (740 MBq) of F-18 fluro-deoxyglucose using a dedicated PET scanner and the standard technique of 2D acquisition with iterative reconstruction and attenuation correction of the images (7). Selected areas with superficially located tumors were imaged with DIRI at the time of staging.

In our study group, 28 tumor sites were identified with CT measurable tumor masses amenable to a single view DIRI acquisition utilizing the BioScanIR® System (OmniCorder Technologies Inc., East Setauket, N.Y.) (10, 12). This system utilizes QWIP FPA detector technology capable of detecting infrared radiation by converting photon flux to electrical signals; the signals are then used to generate images as described above. The system was configured to collect 2048 frames of data over 20 seconds. A specially configured computer system performed real-time capture and storage of data at rates of >25 MB/sec. The individual data files are >250MB in size. This computer system configuration requires at least 2GB of RAM storage, with a computational power equivalent to two 1.2GHz Pentium processors and a 200GB hard drive (10-12). Infrared images were obtained from a distance of 1.5 meters in single projection. Images were stored in the computer memory and processed using dedicated proprietary software to generate color bitmaps for SAA, SSD and FFT as described above. The distribution of the highest 10% of the temperature (T) and temperature modulation (TM) were shown in purple; the next lower T and TM were assigned a red color. These two colors were called "high" T and TM in semi-quantitative evaluations. All remaining colors were called "low" for statistical analysis. Gallium scans were independently evaluated by two board-certified nuclear medicine physicians. The presence or absence of abnormal gallium uptake in regions of "high" or "low" T and TM were evaluated using the Chi-square test. Subsequently thirty 20 × 20 pixel regions of interest were drawn over the tumor masses as well as over 29 areas without tumor masses, and the absolute temperature was evaluated and compared using the Student t-test.

Results

The diagnosis of disease was histologically proven in all 10 Hodgkin's and non-Hodgkin's lymphoma patients. All ten patients underwent gallium-67 imaging and CT. Six of the patients also had F-18 FDG PET. There was good morphologic correlation with Ga-67 scans on visual evaluation of the images. Visual evaluation of scans as utilized in current clinical practice was employed since DIRI imaging is closest to radionuclide techniques due to its functional rather than morphological information it provides. All tumors were found to be highly gallium and FDG avid. The DIRI images collected in a single projection for a single selected region were guided by conventional imaging studies, and had very good morphological correlation of abnormalities when compared with CT and abnormal uptake of radionuclides in tumor masses (Figure 1, 2). The 20 × 20 pixels regions of

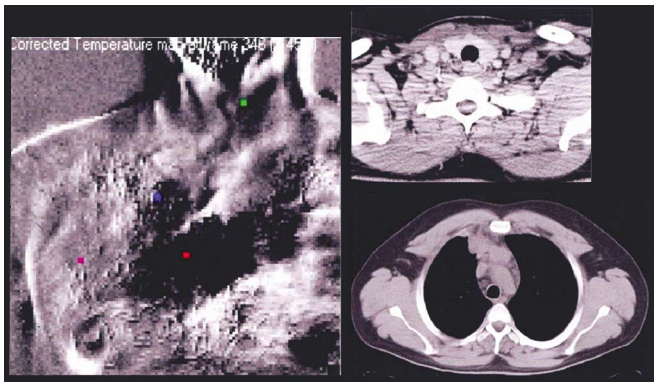

Figure 1a: GC, 29yowm: Newly diagnosed non-Hodgkin's lymphoma with lymphadenopathy in the right neck, supraclavicular regions bilaterally, and mediastinum in retrosternal and paratracheal regions as seen on selected two CT axila cuts over lower neck and upper chest. Left upper panel: DIRI - raw temperature distribution. High temperature over the mediastinum extending to supraclavicular regions bilaterally. (Note color-coded small regions of interest for graphs on Figure 2: blue and red over the tumor, purple over right pectoral muscle, and green over the thyroid.)

Figure 1b: Same patient as Figure 1a: F-18 FDG PET demonstrating lymphadenopathy affecting right lower neck, supraclavicular regions and more extensively mediastinum.

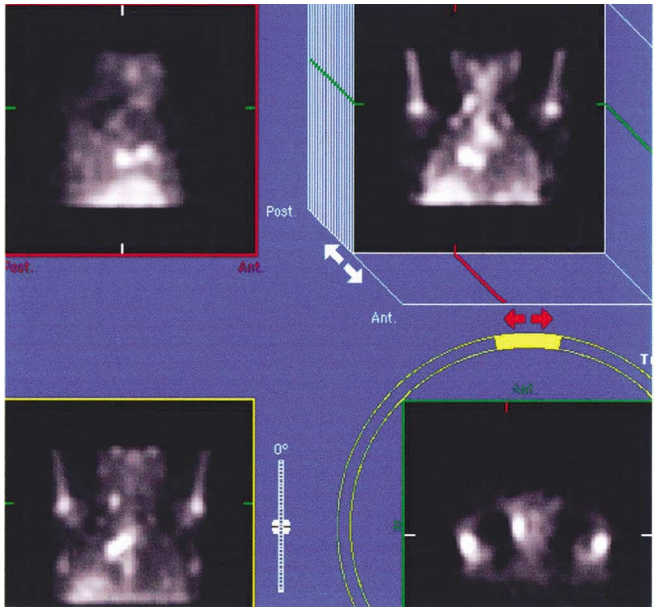

interest placed over the areas of tumor masses detected on CT, radionuclide and DIRI studies showed significantly higher SAA readings compared to sites with no detectable tumors. The SAA over the tumors was 31.786 ± 0.983 as compared to normal tissues with temperature 31.228 ± 0.714 degrees C; t = 2.458, DF = 55, P = .017 (Graph). Areas of high relative SAA (coded as purple and red for highest 20%) corresponded to abnormal gallium-67 deposition, P <0.001, Fisher exact test (Table I). The same very close correlation was observed between high FFT (coded as purple and red for highest 20%) and Ga-67 abnormal uptake, P <0.001, Fisher exact test (Table II). Color coded maps were also generated from the original data sets, evaluating SSD within 2 × 2 pixel areas, reflecting the thermal heterogeneity of tissues. Most tumor masses showed homogeneous temperature distribu-

Graph

Correlation of absolute temperature of skin surface over tumor sites with normal areas.

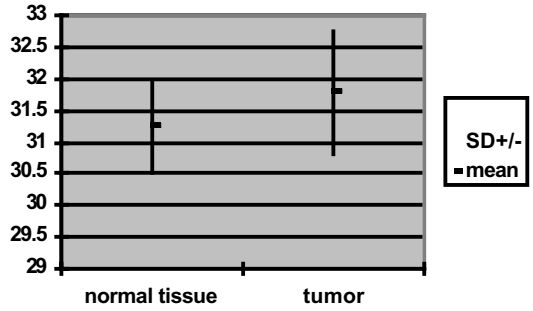

Temperature over tumors 31.78±0.98° C; temperature over normal tissues 31.23 ± 0.71° C.

T = 2.458, DF = 55, P = 0.017.
(20 × 20 pixel ROI, distance 1.5 m, infrared emission 8-10 µm, OmniCorder system, in plane 256 × 256 detector matrix).

Table I

Comparison of sites with abnormal Ga-67 uptake and high temperature on bit-maps.

Gallium-67	LOW temperature	HIGH temperature
Normal	12 (26.7%)	3 (6.7%)
Abnormal	5 (11.1%)	25 (55.6%)
Total:	17 (37.8%)	28 (62.3%)

Fisher exact test: P=<0.001

Table II

Comparison of sites with abnormal Ga-67 uptake and high temperature modulation on bit-maps.

Gallium-67	LOW Temp. Modulation	HIGH Temp. Modulation
Normal	11 (24.4%)	4 (8.9%)
Abnormal	3 (6.6%)	27 (60.0%)
Total:	14 (31.0%)	31 (68.9%)

Fisher exact test: P=<0.001

Figure 1c: Same as Figure 1a,b: Gallium-67 scan demonstrating extensive lymphadenopathy in the neck and chest as PET and DIRI. (Clockwise from upper left: sagital, coronal, volume rendered, and axial images)

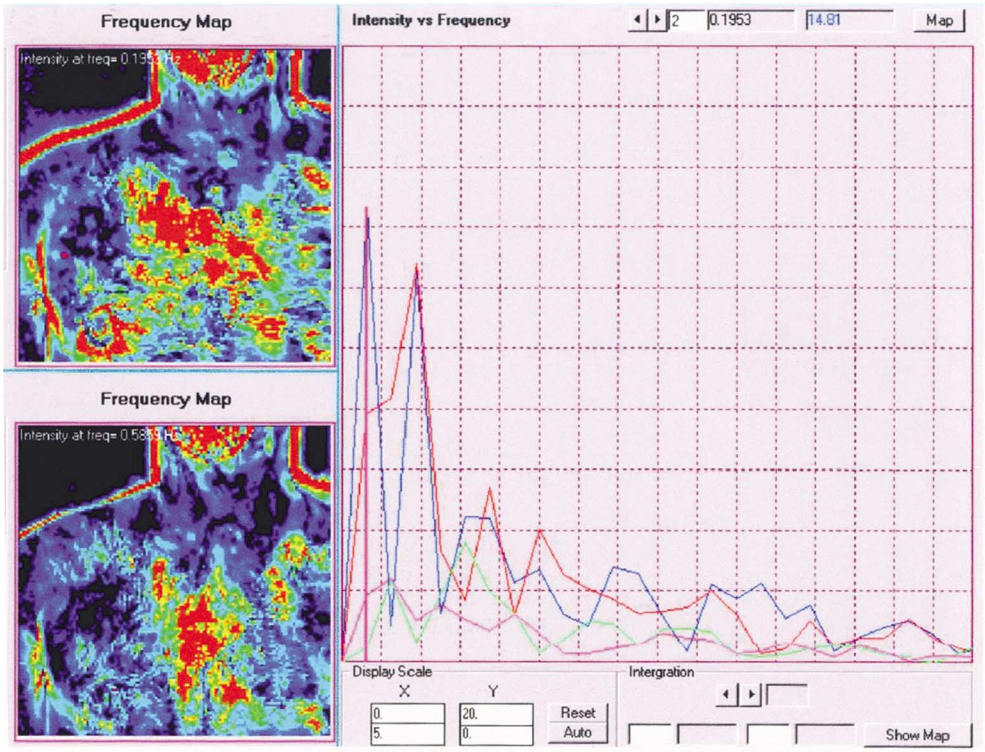

Figure 2: GC, 29 yowm with NHL: (same as Fig. 1): Color panels (anterior view of the chest): Left upper panel showing higher intensity of temperature oscillation in the areas of tumor in the upper mediastinum to the right of the midline investigated selectively for frequency of 0.1953 Hz. Left lower panel is the same area investigated at 0.5859 Hz. These frequencies were identified as the peaks on Fourier transformation of all frequencies in the interval 0-50 Hz depicted on the right hand side. (x axis = frequency, y axis = intensity) Blue and red curves are frequencies over the tumor, green and purple curves are over the pectoral muscle and thyroid. Note a very good correlation with Ga-67 and F-18 FDG PET abnormalities demonstrated on Figure 1.

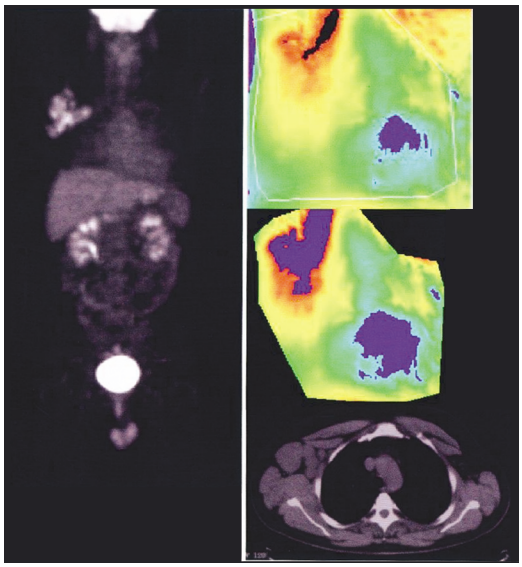

Figure 3: CC, 38yowm: Newly diagnosed Hodgkin's disease (lymphocyte predominant type) with bulky lymphadenopathy in the right axila. Composite image: (**a**) Left panel: F-18 FDG PET. Intense abnormal uptake in the right axila. (**b**) DIRI image, LAO view of the right axila with arm elevated same as on PET image (upper and mid right panels): Discrete area of high temperature and area of high temperature oscilation corresponding to PET abnormality in purple and red. Relatively cold pectoral muscle is light and dark blue. (**c**) Right lower panel: CT axial cut of upper chest with bulky right axilary lymphadenopathy.

tion, with some demonstrating a rim of heterogeneous temperature, but there was no uniform pattern observed.

Discussion

High success rates in the treatment of malignant lymphoma and the availability of alternative treatments increase the demand for accurate staging and early monitoring of therapy response (13, 14). Imaging will play an increasingly important role in this evaluation (3, 5, 14). Conventional imaging, consisting of CT and MRI in combination with radionuclide studies, allows accurate staging and guidance for biopsy (5, 15). These imaging techniques, however, become problematic after treatment begins. In our earlier work we documented the predictive value of the early restaging with the use of gallium-67 in the middle of the treatment (1). Others have suggested the need for even earlier restaging (4, 6, 16). Conventional techniques cannot differentiate residual soft tissue masses from persistant disease (7, 13). The standardization of the technique and the evaluation of radionuclide studies are relatively subjective in the setting of limited residual disease. Also, the cost and availability – as well as the radiation dose – represent additional limitations to repeated use of conventional and gallium-67 imaging at multiple time points during treatment. DIRI may represent a

very important non-invasive, non-contact, inexpensive and easily reproducible alternative, generating direct information about the basic physiology of tissues (10-12, 17). Infrared photon flux emanating from tissue is the by product of metabolic heat production and emission. This is controlled by a variety of physiological and pathologic mechanisms, including systemic and local controls. These include blood perfusion, neurogenic control, local tissue mediators and endothelial receptors. Current imaging generally uses indirect indices of metabolic activity and perfusion. One such parameter, glucose metabolism, has been shown to be very active in lymphomas, as demonstrated by F-18 FDG PET (3, 5, 7). Lesions are usually well perfused, with moderate contrast enhancement on CT after the injection of iodinated contrast, although they do not typically demonstrate the same degree of pathological vasculature known from angiography of sarcomas or some epithelial tumors.

D. S. Kapp *et al*. (25) reported the potential prognostic significance of temperature measurement during treatment. Using probes within the tumors of different histologies – before and during radiotherapy – and hyperthermia, they demonstrated that lower pretreatment temperature and larger difference of temperature before and after treatment were predictive of better local treatment control. Similarly, infrared data in our study was intended to image lymphoma masses at the time of staging to identify the thermo-characteristics of these lesions, which could be used for monitoring the disease during treatment. Changes in infrared flux are probably due to a complex interaction between multiple parameters that are evolving and changing over the course of tumor development and treatment, including the toxic effects of the drugs (10, 12, 22, 25), recruitment of blood vessels and angiogenesis stimulated by the tumors, to name a few. These parameters are currently under intense exploration by many researchers as independent prognostic factors for cancer, and they all very likely contribute to heat distribution and production (12, 22-24).

Conclusion

Raw temperature and temperature modulation measured with DIRI can distinguish lymphoma from adjacent tissues. Infrared body anatomy and physiology need to be further studied to allow refined evaluation of images as well as a better understanding of the quantitative data. Typical patterns may be identified that may allow incorporating this promising functional imaging technique to follow up of patients with malignant lymphoma. Exploring specific frequencies may produce new information about different tumor types, the effects of treatment and the disease state, and will be further refined in larger series in the future.

References

1. Janicek, M., Kaplan, W., Neuberg, D. *et al*. Early Restaging Gallium Scans Predict Outcome in Poor-prognosis Patients with Aggressive Non-Hodgkin's Lymphoma Tereated with High-dose CHOP Chemotherapy. *J. Clin. Oncol. 15*, 1631-1637 (1997).
2. Nyirjesy, I. and Billingsley, F. S. Detection of Breast Carcinoma in a Gynecological Practice. *Obstet. Gynecol. 64*, 747-751 (1984).
3. Delbeke, D. Oncological Applications of FDG PET Imaging. *J. Nucl. Med. 40*, 1706-1715 (1999).
4. Front, D., Bar-Shalom, R., Mor, M. *et al*. Hodgkin's Disease: Prediction of Outcome with Ga-67 Scintigraphy After One Cycle of Chemotherapy. *Radiology 210*, 487-491 (1999).
5. Domke, R. The Use of Gallium-67 in the Follow-up of Lymphoma. *Applied Radiology June*, 6-7 (1999).
6. Front, D., Bar-Shalom, R., Mor, M. *et al*. Aggressive Non-Hodkin's Lymphoma: Early Prediction of Outcome with Ga-67 Scintigraphy. *Radiology 214*, 253-257 (2000).
7. Torizuka, T., Zasadny, K. R., Kinson, P. V. *et al*. Metabolic Response of Non-Hodgkin's Lympoma to I-131-Anti-B1 Radioimmunotherapy: Evaluation with FDG PET. *J. Nucl. Med. 41*, 999-1005 (2000).
8. Kole, A. C., Plaat, B. E. C., Hoekstra, H. J. *et al*. FDG and L-1-C-11-Tyrosine Imaging of Soft Tissue Tumors Before and After Therapy. *J. Nuc. Med. 40*, 381-386 (1999).
9. Hara, T., inagaki, K., Kosaka, N. *et al*. Sensitive Detection of Mediastinal Lymph Node Metastasis of Lung Cancer with C-11 Choline PET. *J. Nuc. Med. 41*, 1507-1513 (2000).
10. Anbar, M., Milescu, L. Hardware and Software Requirements of Clinical DAT. *Infrared Technology and Applications XXV v 3698*, 68-73 (1999).
11. Fauci, M. A., Breiter, R., Cabanski, W. *et al*. Medical Infrared Imaging - Differentiating Facts From Fiction, and the Impact of High Precision Quantum well Infrared Photodetector (QWIP) Camera Systems, and Other Factors, in its Reemergence. *Presented at International QWIP Workshop*, Dana Point, CA, July15, 2000.
12. Anbar, M., Brown, C., Milescu, L. Objective Identification of Cancerous Breasts by Dynamic Area Telethermometry (DAT). *Thermology International 9*, 127-133, 1999.
13. Cheson, B. D., Horning, S. J., Coiffier, B. *et al*. Report of an International Workshop to Standardize Response Criteria for Non-Hodkin's Lymphomas. *J. Clin. Oncol. 17*, 1244-1253 (1999).
14. Shipp, M. A. Prognostic Factors in Aggressive Non-Hodgkin's Lymphoma: Who has "High-risk" Disease? *Blood 83*, 1165-1173 (1994).
15. Nejmeddine, F., Raphael, M., Martin, A. *et al*. Ga-67 Scintigraphy in B-cell Non-Hodgkin's Lymphoma: Correlation of Ga-67 Uptake with Histology and Transferin Receptor Expression. *J. Nucl. Med. 40*, 40-45 (1999).
16. Hoekstra, O. S., Ossenkoppele, G. J., Golding, R. *et al*. Early Treatment Response in Malignant Lymhoma, As Determined by Planar Fluorine-18-fluorodeoxyglucose Scintigraphy. *J. Nuc. Med. 34*, 1706-1710 (1993).
17. Anbar, M., Marino, M. T., Milescu, L. *et al*. Fast Dynamic Area Telethermometry (DAT) of the Human Forearm with Ga/As Quantum Well Infrared Focal Plane Array Camera. *Eur. J. Thermology 7*, 105-118 (1997).
18. Lloyd-Williams, K. Handley RS: Infra-red Thermometry in the Diagnosis of Breast Disease. *Lancet 2*, 1378-1381 (1961).
19. Useki, H. Evaluation of the Thermographic Dignosis of Breast Disease. Relation of Thrmographic Findings and Pathologic Findings of Cancer Growth. *Nippon Gan Chiryo Gakkai Shi 23*, 2687-2695 (1988).
20. Bothmann, G. A. and Kubli, F. Plate Thermography in the Assessment of Changes in the Female Breast. 2. Clinical and Thermographic Results. *Fortschr. Med. 102*, 390-393 (1984).
21. Gautherie, M. and Gros, C. M. Breast Thermography and Cancer

Risk Prediction. *Cancer 45*, 51-56 (1980).
22. Weidner, N., Folkman, J., Pozza, F., Bevilacqua, P., Allred, E. N., Moore, D. H., Meli, S. and Gasparini, G. Tumor Angiogenesis, A New Significant and Independent Prognostic Indicator in Early-stage Breast Carcinoma. *Journal Of The National Cancer Institute 84*, 1875-1887.
23. Gamagami, P. Indirect Signs of Breast Cancer, Angiogenesis Study. in *Atlas of Mammography*, pp, 231-258. Cambridge, MA, Blackwell Science (1996).
24. Ignarro, L. J., Harbison, R. G., Wood, K. S. *et al*. Dissimilarities Between Methylene Blue and Cyanide on Relaxation and Cyclic GMP Formation in Endothelium-intact Intrapulmonary Artery Caused by Nitrogen Oxide-containing Vasodilators and Acetylcholine. *J. Pharmacol. Exp. Ther. 236*, 30-36 (1986).
25. Dimitrakopoulos-Strauss, A., Strauss, L. G., Goldschmidt, H. *et al*. Evaluation of Tumor Metabolism and Multidrug Resistance in Patients with Treated Malignant Lymphomas. *Eur. J. Nucl. Med. 22*, 434-442 (1995).
26. Kapp, D. S., Brown, A. N., Cox, W. *et al*. Temperature Differentials Between Treaatment and Pretreatment Temperatures Correlate with Local Control Following Radiotherapy and Hypothermia. *Int. J. Radiat. Oncol. Biol. Phys. 27*, 331-344 (1993).
27 Button, T. M. *Technical Report to OCT, Initial FFT-DAT with Optimized Collection*. Presented at OCT Meeting, Stony Brook, NY, December 15, 2000.

Date Received: October 7, 2003